Enhancing Pathological Detection and Monitoring in OCT Volumes with Limited Slices using Convolutional Neural Networks and 3D Visualization Techniques

Emilio López-Varela, Noelia Barreira, Nuria Olivier Pascual, and Manuel G. Penedo

Grupo VARPA, Instituto de Investigación Biomédica de A Coruña (INIBIC), Universidade da Coruña, Xubias de Arriba, 84, 15006 A Coruña, Spain
Centro de Investigación CITIC, Universidade da Coruña, 15071 A Coruña, Spain
Servizo de Oftalmoloxía, Complejo Hospitalario Universitario de Ferrol (CHUF), Av. da Residencia S/N, Ferrol 15405, Spain
Correspondence: e.lopezv@udc.es

DOI: *https://doi.org/10.17979/spudc.000024.23*

Abstract: Optical Coherence Tomography (OCT) is a non-invasive imaging technique with a crucial role in the monitoring of a wide range of diseases. In order to make a good diagnosis it is essential that clinicians can observe any subtle changes that appear in the multiple ocular structures, so it is imperative that the 3D OCT volumes have good resolution in each axis. Unfortunately, there is a trade-off between image quality and the number of volume slices. In this work, we use a convolutional neural network to generate the intermediate synthetic slices of the OTC volumes and we propose a few variants of a 3D reconstruction algorithm to create visualizations that emphasize the changes present in multiple retinal structures to aid clinicians in the diagnostic process.

1 Introduction

Optical Coherence Tomography (OCT) is a non-invasive imaging modality of great importance for the diagnosis and ongoing monitoring of a wide range of ocular and systemic diseases. By providing an accurate examination of the three-dimensional anatomy of the eye, OCT facilitates the early detection and monitoring of diseases such as central serous chorioretinopathy López-Varela et al. (2023b), diabetic macular edema Vidal et al. (2020), age-related macular degeneration López-Varela et al. (2022), hypertension, and even multiple sclerosis Garcia-Martin et al. (2021); López-Varela et al. (2022). These diseases have a profound impact on the lives of patients, ranging from irreversible visual impairment to gradual loss of mobility. Hence, the timely and accurate diagnosis of these conditions becomes essential Medeiros et al. (2005).

The effectiveness of OCT in diagnosing disease depends on the ability of clinicians to quickly detect even the most subtle changes in ocular structures. The task of visualizing these alterations in the discrete 2D slices that constitute each OCT volume is labor-intensive and time-consuming. Moreover, this method is prone to subjectivity and relies heavily on the experience of the clinician, who must extrapolate three-dimensional structural changes from observations of individual slices Apostolopoulos et al. (2017). In contrast, 3D reconstructions provide a complete and accurate visualization of all structures in the OCT volume at a glance. This mode of visualization substantially streamlines the workflow of the clinician, increasing the robustness and accuracy of diagnoses and significantly reducing the workload and, consequently, the direct and indirect costs incurred by healthcare services.

In order to use 3D visualization effectively, it is imperative that 3D OCT volumes have good resolution in each axis. Unfortunately, due to the acquisition mechanism of OCT, there is a trade-off between the image quality and the number of volume slices, which limits the resolution in some of the axes and forces to choose different settings of these parameters depending on the objective of the study Huang et al. (1991). Many routine clinical studies opt for OCT volumes composed of a limited number of high-resolution images, which decreases the effectiveness of 3D visualizations in the diagnostic process by profoundly reducing the resolution of the cube in the slice dimension as shown in Figure 1.

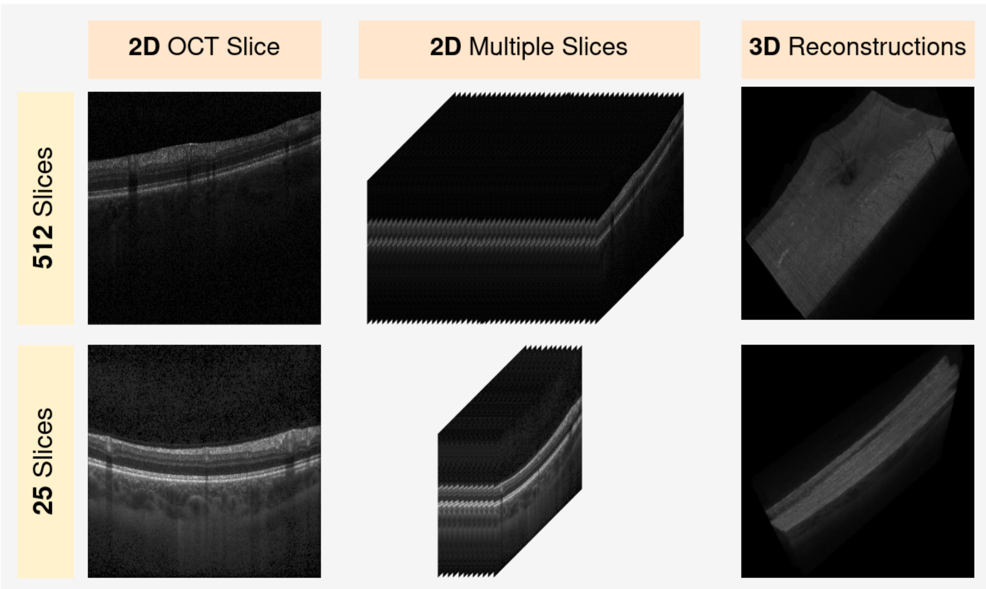

Figure 1: Two OCT cubes with different number of slices. The 2D representation of a single image and a 3D reconstruction of the volume are shown.

It is therefore of great interest to create a system capable of synthesising the intermediate images between adjacent slices in order to increase the cross-sectional resolution of the volume. As a consequence, some papers have begun to propose different initial approaches based on neural networks to solve similar problems in OCT López-Varela et al. (2023a) or in other medical imaging modalities such as magnetic resonance imaging Peng et al. (2020). In addition to having an OCT volume with good resolution, it is essential that the 3D reconstruction algorithm produces a visualization where each of the analyzed diagnostic features is accurately identified. Structural alterations, such as the presence of fluid, can be discerned in a standard reconstruction, but it is challenging for a clinician to estimate subtle changes in a more general feature, such as layer thickness, at a glance. These types of changes are much better visualized using alternative visualization systems, such as depth-based heatmaps, in combination with complementary techniques like structure segmentation. Therefore, there is a paramount interest in designing and creating a system that employs a combination of multiple visualizations that complement each other, emphasizing different characteristics of the analyzed structure.

Given all these problems, in this work, we use a convolutional neural network trained in an unsupervised manner, which leverages information from adjacent slices to generate the intermediate synthetic slices of the volume. To fully exploit this enhanced resolution cube and accurately monitor changes in multiple diagnostic biomarkers, several variants of a 3D reconstruction algorithm are proposed. These algorithms generate diverse visualizations with complementary functions, highlighting changes in various retinal structures, including layer thickness. These visualizations hold the potential to significantly aid clinicians in the diagnostic process, emphasizing the paramount importance of a comprehensive visual approach in medical diagnostics.

2 Materials and Methods

A complete diagram showing the different processes of the proposed diagnostic visualization system can be observed in Figure 2. To assess the effectiveness of the proposed visualization system, in this work, we use the dataset and the network architecture presented in López-Varela et al. (2023a). This dataset consists of 42 OCT cubes obtained using two identical Spectralis R OCT capture devices from Heidelberg Engineering. These cubes encompass three distinct categories of OCT volumes captured by different configurations commonly used in clinical practice and have a limited number of slices. This characteristic significantly degrades 3D visualizations, highlighting the indispensability of the generative network for enhancing the visualization quality. In addition to the generative network, and as a complement to our visualization system, we employ a segmentation network trained to segment the multiple layers of the retina. This segmentation network is a variation of the UNet Ronneberger et al. (2015) with the classic encoder-decoder structure. The segmentation masks generated by this network enable us to individually fine-tune the appearance of each layer within the 3D visualization, with the purpose of emphasizing the most significant diagnostic features.

Finally, to establish a 3D reconstruction algorithm to exploit the OCT volumes with enhanced resolution, we have adapted and improved the reconstruction algorithm proposed in López-Varela et al. (2022), creating four complementary variants that highlight different aspects of the analyzed layers. These variants are obtained by altering three parts of the reconstruction methodology: the voxel values of each OCT volume, the color-opacity transfer function, and the composition system of the ray casting algorithm.

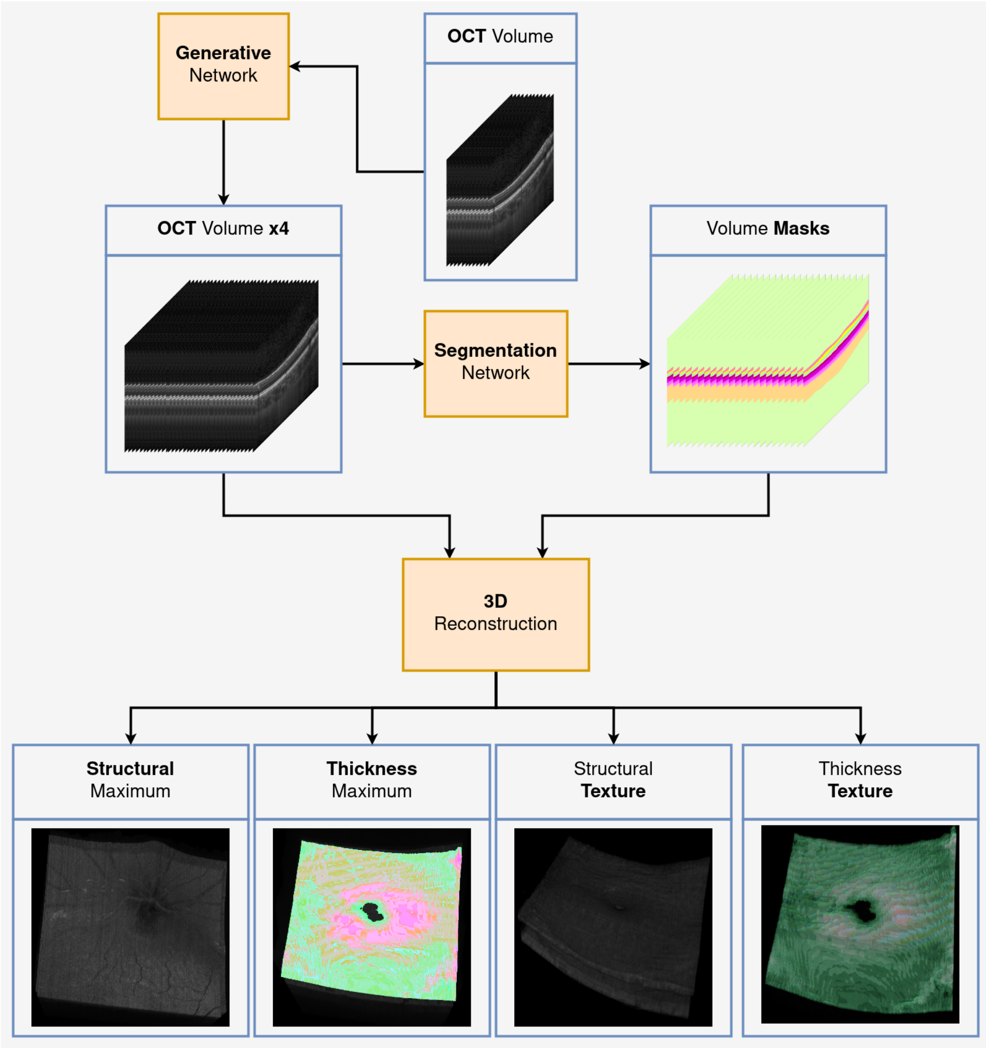

Figure 2: Diagram of the diagnostic visualization system.

- **Structural Maximum**: To obtain this variant, the voxel values are adjusted using the segmentation mask of the analyzed structure. This way, the graylevel intensities of voxels belonging to the layer are compressed into the range [20, 256], while values that do not belong to it are compressed into the range [0, 19]. The opacity transfer function is adjusted to increase transparency for values outside the layer in the range [0, 19], and the maximum intensity is used as the composition system.
- **Thickness Maximum**: In addition to the processing applied in 'Structural Maximum', the intensities of voxels belonging to the layer are adjusted to obtain a heat map indicating the thickness. To achieve this, a distance transform is applied to the mask cube. The result of applying the distance transform is a volume where the graylevel intensities of points inside the layer are changed to show the distance to the closest boundary from each point. The voxels of the original cube are modified based on the distance-transformed cube to obtain an estimation of the layer thickness. Lastly, the transfer function is adjusted to apply a Red-Green color scale based on the intensity value of

each voxel.

- **Structural Texture**: In addition to the processing applied in 'Structural Maximum', a front-to-back composition scheme using alpha blending is used as the composition system.
- **Thickness Texture**: In addition to the processing applied in 'Thickness Maximum', the opacity gradient transfer function is modified according to the distance-transformed cube, and the composition scheme is applied as the composition system.

3 Results and Discussion

In this section, we present the results obtained by employing our visualization methodology on OCT volumes with a low number of slices. To assess the utility of each component comprising our system, we display the four proposed visualization variants before and after applying the generative network to a 25-slice OCT volume. Figure 3 illustrates this effect in two planes of two distinct layers of the retina, the retinal nerve fibre layer (RNFL) and the ganglion cell layer (GCL). To focus the visualization on these layers, we utilize the masks obtained through the proposed segmentation network. The use of this network enables the individual extraction and emphasis of each clinically significant structure.

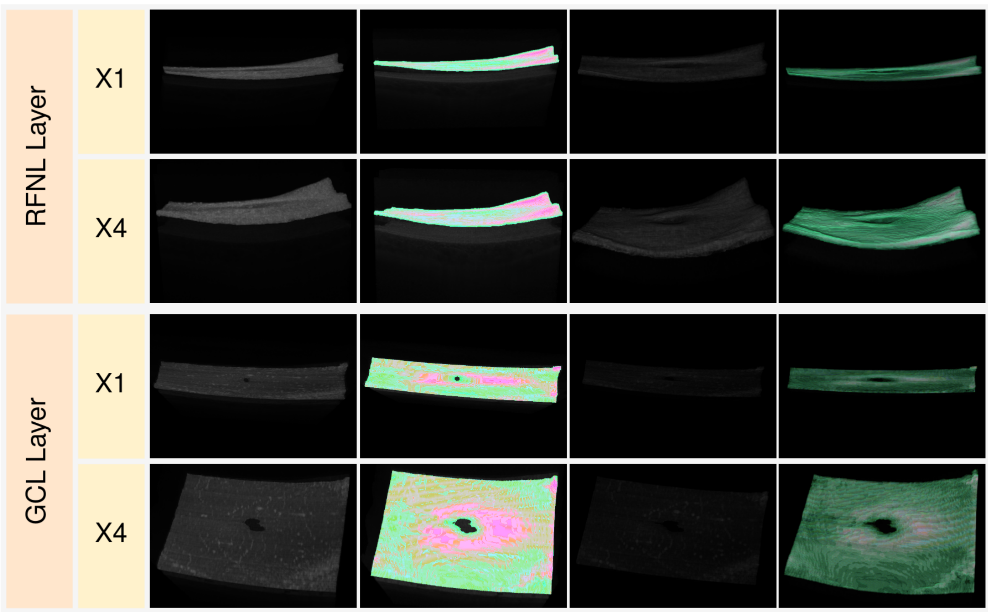

Figure 3: Sample figure caption.

In general, it can be observed that the use of the generative network is essential for achieving accurate reconstruction that displays the details of each layer. When using the original OCT volume, the lack of resolution prevents us from discerning any kind of detail in the layer, such as blood vessels or the macular hole. It even hinders our ability to distinguish the shape and thickness of the structure. Conversely, these characteristics are clearly distinguishable when using the enhanced OCT volumes. These results reinforce the conclusions obtained in López-Varela et al. (2023a), where the realism of enhanced OCT volumes and the utility of synthetic layer generation were validated by clinical experts.

Each variant of the reconstruction algorithm emphasizes a feature with diagnostic significance. The first variant allows us to observe the internal details of the layer clearly, such as blood vessels, and provides good contrast to distinguish the multiple structures that compose the layer at different depths. In contrast to this, the third variant shows the surface details of the layer, allowing for precise observation of its exact shape, which helps identify any malformations. The second and fourth variants display the thickness of the layer on a green-red color scale, enabling the observation of pathological thickening or thinning. Detecting these thickness changes in the layers is crucial for diagnosing and monitoring many diseases, such as multiple sclerosis, making the contribution of these two visualizations to the system significant. These types of visualizations also assist in visualizing other pathological structures, such as fluid accumulation, making their use versatile and of general nature. The diagnostic system as a whole enables precise visualization and differentiation of the multiple pathological features present in the ocular structure at a glance. Therefore, we can conclude that this system has great potential to assist clinicians and significantly lighten the diagnostic workload.

Acknowledgements

This research was funded by Government of Spain, Ministerio de Ciencia e Innovación y Universidades, Government of Spain, RTI2018-095894-B-I00 research project; Ministerio de Ciencia e Innovación, Government of Spain through the research projects with reference PID2019-108435RB-I00, PDC2022-133132-I00 and TED2021-131201B-I00; Consellería de Cultura, Educación e Universidade, Xunta de Galicia through the Grupos de Referencia Competitiva, grant ref. ED431C 2020/24; CITIC, as Research Center accredited by Galician University System, is funded by "Consellería de Cultura, Educación e Universidade from Xunta de Galicia", supported in an 80% through ERDF Funds, ERDF Operational Programme Galicia 2014-2020, and the remaining 20% by "Secretaría Xeral de Universidades", grant ref. ED431G 2019/01. Emilio López Varela acknowledges its support under FPI Grant Program through PID2019-108435RB-I00 project.

Bibliography

S. Apostolopoulos, S. De Zanet, C. Ciller, S. Wolf, and R. Sznitman. Pathological oct retinal layer segmentation using branch residual u-shape networks. In *Medical Image Computing and Computer Assisted Intervention- MICCAI 2017: 20th International Conference, Quebec City, QC, Canada, September 11-13, 2017, Proceedings, Part III 20*, pages 294–301. Springer, 2017.

E. Garcia-Martin, M. Ortiz, L. Boquete, E. M. Sánchez-Morla, R. Barea, C. Cavaliere, E. Vilades, E. Orduna, and M. J. Rodrigo. Early diagnosis of multiple sclerosis by oct analysis using cohen's d method and a neural network as classifier. *Computers in Biology and Medicine*, 129: 104165, 2021.

D. Huang, E. A. Swanson, C. P. Lin, J. S. Schuman, W. G. Stinson, W. Chang, M. R. Hee, T. Flotte, K. Gregory, C. A. Puliafito, et al. Optical coherence tomography. *Science*, 254(5035):1178–1181, 1991.

E. López-Varela, P. L. Vidal, N. O. Pascual, J. Novo, and M. Ortega. Fully-automatic 3d intuitive visualization of age-related macular degeneration fluid accumulations in oct cubes. *Journal of Digital Imaging*, pages 1–12, 2022.

E. López-Varela, N. Barreira, N. O. Pascual, M. R. A. Castillo, and M. G. Penedo. Generation of synthetic intermediate slices in 3d oct cubes for improving pathology detection and monitoring. *Computers in Biology and Medicine*, 163:107214, 2023a.

E. López-Varela, J. de Moura, J. Novo, J. I. Fernández-Vigo, F. J. Moreno-Morillo, and M. Ortega. Fully automatic segmentation and monitoring of choriocapillaris flow voids in octa images. *Computerized Medical Imaging and Graphics*, 104:102172, 2023b.

E. López-Varela, N. Barreira, N. O. Pascual, E. G. Ben, S. R. Cid, and M. G. Penedo. Fully automatic segmentation of the choroid in non-edi oct images of patients with multiple sclerosis. *Procedia Computer Science*, 207:726–735, 2022. Knowledge-Based and Intelligent Information and Engineering Systems: Proceedings of the 26th International Conference KES2022.

F. A. Medeiros, L. M. Zangwill, C. Bowd, R. M. Vessani, R. Susanna Jr, and R. N. Weinreb. Evaluation of retinal nerve fiber layer, optic nerve head, and macular thickness measurements for glaucoma detection using optical coherence tomography. *American journal of ophthalmology*, 139(1):44–55, 2005.

C. Peng, W.-A. Lin, H. Liao, R. Chellappa, and S. K. Zhou. Saint: spatially aware interpolation network for medical slice synthesis. In *Proceedings of the IEEE/CVF Conference on Computer Vision and Pattern Recognition*, pages 7750–7759, 2020.

O. Ronneberger, P. Fischer, and T. Brox. U-net: Convolutional networks for biomedical image segmentation. In *Medical Image Computing and Computer-Assisted Intervention–MICCAI 2015: 18th International Conference, Munich, Germany, October 5-9, 2015, Proceedings, Part III 18*, pages 234–241. Springer, 2015.

P. L. Vidal, J. de Moura, M. Díaz, J. Novo, and M. Ortega. Diabetic macular edema characterization and visualization using optical coherence tomography images. *Applied Sciences*, 10(21): 7718, 2020.